Food Chemistry 317 (2020) 126397

Contents lists available at ScienceDirect

Food Chemistry

journal homepage: www.elsevier.com/locate/foodchem

# Fast-dissolving antioxidant curcumin/cyclodextrin inclusion complex electrospun nanofibrous webs

Asli Celebioglu*, Tamer Uyar*

*Department of Fiber Science & Apparel Design, College of Human Ecology, Cornell University, Ithaca, NY 14853, United States*

ARTICLE INFO

*Keywords:*
Curcumin
Cyclodextrin
Electrospinning
Nanofibers
Antioxidant activity
Fast-dissolving
Food supplement

ABSTRACT

Curcumin/Hydroxypropyl-beta-Cyclodextrin (HP-β-CyD) and Curcumin/Hydroxypropyl-gamma-Cyclodextrin (HP-γ-CyD) inclusion complex nanofibrous webs were produced using electrospinning technique for the purpose of orally fast-dissolving antioxidant food supplement. Curcumin was totally preserved without any loss during the electrospinning process. The aqueous solutions of curcumin/HP-β-CyD and curcumin/HP-γ-CyD were yielded uniform fiber morphology with ~200 nm and ~900 nm average fiber diameter, respectively. Both Curcumin/CyD webs were produced in the form of free-standing and flexible character. Curcumin is a natural bioactive compound with poor water-solubility, however, the phase solubility test and dissolution/disintegration tests (water and artificial saliva) revealed that the water-solubility of curcumin was prominently improved by inclusion complexation with CyD. The antioxidant effect of curcumin in Curcumin/CyD webs was also enhanced due to higher solubility of curcumin by CyD inclusion complex. The results showed that HP-γ-CyD is significantly more effective than HP-β-CyD in order to enhance the solubility and antioxidant property of curcumin in Curcumin/CyD webs.

## 1. Introduction

Food bioactive compounds such as essential oils, antioxidants, vitamins, and flavors, etc. possess important functions, yet, such bioactive compounds suffer from low stability against temperature, light, oxygen, and they are poorly water-soluble having low bioavailability. Therefore, encapsulation of bioactive compounds offers longer shelf-life by improving their stability, water-solubility and bioavailability (Dias, Ferreira, & Barreiro, 2015). Various encapsulation methods such as emulsion, extrusion, co-precipitation, coacervation, spray-drying, freeze-drying can be applied for encapsulating food bioactive compounds (Dias et al., 2015). Recently, the electrohydrodynamic processes such as electrospraying and electrospinning have shown to be very promising and emerging methods in which food bioactive compounds can be effectively encapsulated within suitable biopolymer matrices (Bhushani & Anandharamakrishnan, 2014). In the case of electrospraying, micro and nano particles are formed whereas nanofibers having diameters of sub-microns down to hundred nanometers are formed in the case of electrospinning (Bhushani & Anandharamakrishnan, 2014).

The electrospun nanofiber matrices encapsulating bioactive compounds have shown promises in food and food packaging applications (Leidy & Ximena, 2019). The nanofibers are electrospun as nonwoven mat/web form having lightweight, flexible and self-standing features along with very large surface area and highly porous structure. The electrospun nanofibrous mats/webs made of water-insoluble biopolymers encapsulating bioactive compounds are suitable for food packaging applications (Torres-Giner, Busolo, Cherpinski, & Lagaron, 2018). On the other hand, the electrospun nanofibrous mats/webs produced from edible hydrophilic biopolymers encapsulating food bioactive compounds would readily dissolve in water, which can be very favorable for fast-dissolving delivery systems (Yu, Li, Williams, & Zhao, 2018). In our recent studies, we have shown that highly water-soluble fast-dissolving nanofibrous webs/mats can be produced from purely cyclodextrin inclusion complexes of various food bioactive compounds such as flavors (Celebioglu, Kayaci-Senirmak, İpek, Durgun, & Uyar, 2016; Yildiz, Celebioglu, Kilic, Durgun, & Uyar, 2018), essential oils (Aytac, Yildiz, Kayaci-Senirmak, Tekinay, & Uyar, 2017; Celebioglu, Yildiz, & Uyar, 2018; Yildiz, Kilic, Durgun, & Uyar, 2019) and vitamins (Celebioglu & Uyar, 2017) by electrospinning. Cyclodextrins (CyDs) are cyclic oligosaccharides produced from starch, which are used in food industry due to their molecular encapsulation capability by inclusion complexation (Marques, 2010). CyDs enhance the water-solubility and bioavailability, mask the bitter taste, control the release, extend the shelf-life and prevent the loss of such food bioactive compounds by forming inclusion complexes (Marques, 2010). Therefore, electrospun

* Corresponding authors.
*E-mail addresses:* ac2873@cornell.edu (A. Celebioglu), tu46@cornell.edu (T. Uyar).

https://doi.org/10.1016/j.foodchem.2020.126397
Received 6 October 2019; Received in revised form 20 January 2020; Accepted 10 February 2020
Available online 11 February 2020
0308-8146/ 

nanofibrous webs/mats of CyD inclusion complexes with bioactive compounds would be quite promising for food applications.

Curcumin is a naturally occurring polyphenol isolated from the rhizome of turmeric (*Curcuma longa*) as a yellow colored powder compound. Curcumin is a highly effective bioactive compound and it has wide range of pharmacological activities, such as anticancer, anti-inflammatory, antimicrobial, antidiabetic and antioxidant properties (Rauf, Imran, Orhan, & Bawazeer, 2018). Therefore, curcumin has been studied for the treatment of diseases such as cancer, cardiovascular, diabetes, neurological disorders and Alzheimer's disease (Rauf et al., 2018). Curcumin is also widely used in food industry as an herbal food supplement, spice, food preservative, flavoring and coloring agent apart from its application in pharmaceutics as a therapeutic agent (Rauf et al., 2018; Stanić, 2018). Curcumin is very beneficial due to its extensive biological and pharmacological activities, yet, it is a water-insoluble hydrophobic compound, and therefore, it has extremely low bioavailability which limits its benefits (Rauf et al., 2018; Stanić, 2018). Nonetheless, it has been shown that solubility and bioavailability of the curcumin can be dramatically improved by using CyD as a complexing agent (Aytac & Uyar, 2017; Jahed, Zarrabi, Bordbar, & Hafezi, 2014; Yu et al., 2018). Even, Curcumin/CyD inclusion complex systems obtained using hydroxy-propylated CyD derivates can provide biocompatibility for the oral (Li et al., 2018), ocular (Maharjan et al., 2019) and transdermal (Sun et al., 2014) treatments. The encapsulation of curcumin into polymeric nanofiber matrix by electrospinning for the purpose of wound dressing (Pankongadisak, Sangklin, Chuysinuan, Suwantong, & Supaphol, 2019), food (Deng, Kang, Liu, Feng, & Zhang, 2017) and food packaging (Alehosseini, Gómez-Mascaraque, Martínez-Sanz, & López-Rubio, 2019; Wang et al., 2019) applications have been reported. In addition, there are also very few studies regard to electrospun polymeric nanofibers encapsulating Curcumin/CyD inclusion complexes in which CyDs are shown to be quite functional for the controlled release and improved solubility of curcumin (Amiri & Rahimi, 2019; Aytac & Uyar, 2017). Nevertheless, to the best of our knowledge, no study has been reported so far related to electrospinning of nanofibers from purely Curcumin/CyD inclusion complexes for the purpose of developing orally fast-dissolving food supplements.

In this study, we were able to achieve electrospinning of Curcumin/CyD nanofibers by using water as a solvent (Fig. 1). The use of water for the electrospinning of CyD inclusion complexes offers great advantage especially for food applications, on the other hand, the use of organic solvent is a common choice for the electrospinning since most of the polymeric carrier matrix and curcumin are only soluble in organic solvents (Alehosseini et al., 2019; Deng et al., 2017; Pankongadisak et al., 2019). Here, we have chosen highly water-soluble CyD types (hydroxypropyl-beta-cyclodextrin (HP-β-CyD) and hydroxypropyl-gamma-cyclodextrin (HP-γ-CyD)) (Fig. 1a) to form inclusion complexes with curcumin, CyDs (HP-β-CD and HP-γ-CD) act as a molecular encapsulating agent for curcumin and a carrier matrix for the electrospinning. The electrospinning of nanofibers solely from CyD inclusion complex systems without using additional polymeric matrix provides several advantages over the electrospinning of polymeric systems. For example, hydroxypropylated CyDs are highly water-soluble compare to polymeric materials, hence, nanofibers solely electrospun from CyD inclusion complexes would dissolve instantly, in addition, CyDs significantly enhance the water-solubility of hydrophobic bioactive agents by inclusion complexation. In this study, the aqueous solutions of Curcumin/HP-β-CyD and Curcumin/HP-γ-CyD inclusion complexes were successfully prepared and then electrospinning process was performed to produce nanofibers in the form of nanofibrous webs (Fig. 1). Further, we have performed morphological and the detailed structural characterizations of Curcumin/CyD nanofibrous webs. The solubility/dissolution/disintegration profile of Curcumin/CyD nanofibrous webs were studied, as well. The antioxidant activity of Curcumin/HP-β-CyD and Curcumin/HP-γ-CyD inclusion complex nanofibers were also comparatively examined with curcumin powder.

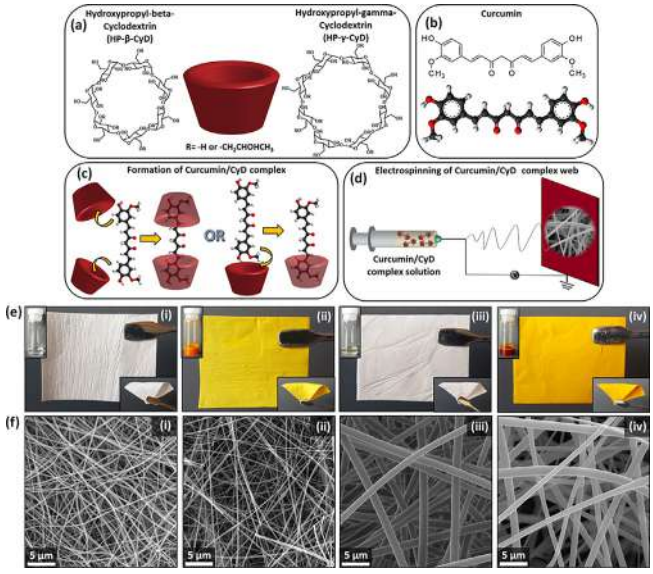


**Fig. 1.** The chemical structure of (a) HP-β-CyD and HP-γ-CyD, and (b) curcumin. (c) The schematic representation of inclusion complex formation between curcumin and CyD molecules, (d) and the electrospinning of Curcumin/CyD webs. (e) The photographs of electrospinning solutions and the ultimate nanofibrous webs and (f) SEM images of (i) HP-β-CyD web, (ii) Curcumin/HP-β-CyD web, (iii) HP-γ-CyD web and (iv) Curcumin/HP-γ-CyD web.

## 2. Materials and methods

### 2.1. Materials

Hydroxypropyl-beta-cyclodextrin (HP-β-CyD) (Cavasol W7 HP, DS: ~0.9) and Hydroxypropyl-gamma-cyclodextrin (HP-γ-CyD) (Cavasol W8 HP Pharma, DS: ~ 0.6) were kindly supplied by Wacker Chemie AG (USA) for laboratory studies. Curcumin (98%, Acros), methanol (≥99.8% (GC), Sigma Aldrich), 2,2-diphenyl-1-picrylhydrazyl (DPPH, ≥97%, TCI America), dimethyl sulfoxide (DMSO, > 99.9%, Sigma Aldrich), sodium chloride (NaCl, > 99%, Sigma Aldrich), potassium phosphate monobasic ($KH_2PO_4$, ≥99.0%, Fisher Chemical), sodium phosphate dibasic heptahydrate ($Na_2HPO_4$, 98.0–102.0%, Fisher Chemical), o-phosphoric acid (85% (HPLC), Fisher Chemical), deuterated dimethylsulfoxide (*d6*-DMSO, 99.8%, Cambridge Isotope) and phosphate buffered saline tablet (PBS, Sigma Aldrich) were purchased and used without further purification. High-quality distilled water was used from the Millipore Milli-Q ultrapure water system (Millipore, USA).

### 2.2. Methods

#### 2.2.1. Preparation of electrospinning solutions and electrospinning process

The highly concentrated (180% (w/v)) and clear solutions of hydroxypropyl-beta-cyclodextrin (HP-β-CyD) and hydroxypropyl-gamma-cyclodextrin (HP-γ-CyD) were prepared in distilled water (0.5 mL). Afterwards, curcumin powder was added to both HP-β-CyD and HP-γ-CyD solutions separately. Firstly, Curcumin/CyD aqueous systems having 1/2 M ratio was prepared, however the system was failed to be electrospun. Then, Curcumin/CyD aqueous systems having 1/4 M ratio which correspond to the ~6.0% (w/w, with respect to total sample amount) of curcumin content in Curcumin/CyD webs were optimized for the further study. The Curcumin/CyD aqueous systems were stirred for 24 h at 60 °C in order to form inclusion complexes. The Curcumin/CyD were cooled down to room temperature prior the electrospinning process. The pristine HP-β-CyD and HP-γ-CyD webs were also electrospun for the comparative studies. The defect-free morphology of pristine CyD webs was guaranteed by electrospinning of 200% CyD (w/v)

concentration in aqueous solution prepared using 0.5 mL distilled water.

The electrospinning of nanofibrous webs was carried out using electrospinning equipment (Spingenix, model: SG100, Palo Alto, USA). The solution of HP-β-CyD, HP-γ-CyD, Curcumin/HP-β-CyD and Curcumin/HP-γ-CyD was loaded in a plastic syringe fixed with 23 G metal needle, separately. Then, solutions were forced through the needle using a syringe pump with the flow rate of 0.5 mL/h. A grounded metal collector was wrapped with a piece of aluminum foil and located at 15 cm from the tip of the needle in order to collect the webs by applying stable voltage of 15 kV using high voltage power supply. The ambient conditions of temperature and humidity were recorded as 20 °C and 55%, respectively during the electrospinning process. For comparison, the physical mixture of Curcumin/HP-β-CyD and Curcumin/HP-γ-CyD system were prepared, as well. In order to obtain Curcumin/CyD physical mixture having the same molar ratio of 1/4 with Curcumin/CyD nanofibrous webs, the definite amount of curcumin powder (~2 mg) was precisely weighted into two separate glass vials. Afterwards, the pristine HP-β-CyD and HP-γ-CyD nanofibrous web (~30 mg) were separately added to these glass vials and mixed using metal spatula until homogenous blends were obtained.

#### 2.2.2. Solution properties

The conductivity of the electrospinning solutions was determined using conductivity-meter (FiveEasy, Mettler Toledo, USA) at room temperature. The viscosity of the same solutions was measured using a rheometer (AR 2000 rheometer, TA Instrument, USA) fitted with 20 mm cone/plate accessory (CP 20-4 spindle type, 4°) under the shear rate range of 0.01–1000 $s^{-1}$ at 22 °C.

#### 2.2.3. Morphology analysis

The morphological investigation of HP-β-CyD, HP-γ-CyD, Curcumin/HP-β-CyD and Curcumin/HP-γ-CyD webs were performed using scanning electron microscope (SEM, Tescan MIRA3, Czech Republic). The small piece of nanofibrous webs were fixed onto SEM stubs and sputter-coated with thin layer of Au/Pd prior the examination. The operating parameters of working distance and accelerating voltage were set to 10 mm and 10 kV, respectively for the SEM imaging. The representative images were taken at magnification of 10.0 kx. The average fiber diameter (AFD) of nanofibers was determined by the measurement of several fibers (~100) using ImageJ software and the results are given as the average diameter ± standard deviation.

#### 2.2.4. Phase solubility profile of Curcumin/CyD systems

Phase solubility study of Curcumin/HP-β-CyD and Curcumin/HP-γ-CyD system was performed applying the previously reported technique (Higuchi & Connors, 1965). The excess amount of curcumin and CyD powder with an increasing concentration from 0 to 20 mM were put into glass vials, separately then 5 mL of water was added to each vial. The sealed vials were shaken for 24 h on incubator shaker at 25 °C and 450 rpm by shielding from the light sources. After incubation, the suspensions were filtered with 0.45 μm PTFE filter (Thermo Scientific, Target2). The filtered aliquots were diluted with an appropriate amounts of phosphate buffer saline solution (PBS; pH 7.4) before the measurements of UV–Vis-spectroscopy (PerkinElmer, Lambda 35), in order to stabilize the pH of the solutions at around 7.4. The experiments were performed in triplicate (n = 3) and the average absorption results were used in order to plot the phase solubility diagrams. The binding constants (Ks) were calculated from the following equation;

$$Ks = slope/S_0(1-slope) \quad (1)$$

where $S_0$ is the intrinsic solubility of curcumin (~8 μM) (Yadav, Suresh, Devi, & Yadav, 2009) in the absence of CyD.

#### 2.2.5. Proton nuclear magnetic resonance spectroscopy

In order to calculate the molar ratio between curcumin and CyD in Curcumin/HP-β-CyD and Curcumin/HP-γ-CyD webs, nuclear magnetic resonance spectrometer (Bruker AV500, with autosampler) was used at 25 °C. Prior the measurements, Curcumin powder, HP-β-CyD web, HP-γ-CyD web, Curcumin/HP-β-CyD web and Curcumin/HP-γ-CyD web were dissolved in *d6*-DMSO at the sample concentration of 70 g/L and proton nuclear magnetic resonance ($^1$H NMR) spectra were recorded upon 16 scans. Mestranova software was used to get the integration of chemical shifts ($\delta$, ppm) which were considered for the calculations. The $-CH_3$ peak of CyD at 1.03 ppm and protons of curcumin between 6.50 and 8.00 ppm were used in order to calculate the molar ratios of Curcumin/HP-β-CyD and Curcumin/HP-γ-CyD webs.

#### 2.2.6. Encapsulation efficiency

In order to calculate the encapsulation efficiency (%), certain amount of Curcumin/HP-β-CyD web and Curcumin/HP-γ-CyD web were dissolved in dimethyl sulfoxide (DMSO) and the curcumin content in webs were determined using UV–Vis-spectroscopy. The calibration curve of curcumin in DMSO showed linearity and acceptability with $R^2 \geq 0.99$. The experiments were performed three times and results were expressed as mean ± standard deviation. The encapsulation efficiency (%) (EE) was calculated by the following equation:

$$\text{Encapsulation efficiency}\,(\%)\,(EE) = Ce/Ct \times 100 \quad (2)$$

where Ce is the concentration of encapsulated curcumin and Ct is the initial concentration of curcumin in webs.

#### 2.2.7. The Fourier transform infrared spectroscopy

The Fourier transform infrared (FT-IR) spectra of Curcumin powder, HP-β-CyD and HP-γ-CyD webs, Curcumin/HP-β-CyD and Curcumin/HP-γ-CyD webs, Curcumin/HP-β-CyD, and Curcumin/HP-γ-CyD physical mixtures were recorded using Attenuated total reflectance Fourier transform infrared (ATR-FT-IR) spectrometer (PerkinElmer, USA). The spectra were taken between 4000 and 600 $cm^{-1}$ at a resolution of 4 $cm^{-1}$ and upon 64 scans.

#### 2.2.8. X-ray diffraction

The X-ray diffraction pattern of Curcumin powder, HP-β-CyD and HP-γ-CyD webs, Curcumin/HP-β-CyD and Curcumin/HP-γ-CyD webs, Curcumin/HP-β-CyD, and Curcumin/HP-γ-CyD physical mixtures were determined using X-ray diffractometer (XRD, Bruker D8 Advance ECO). Prior the measurements, the voltage and current were set to 40 kV and 25 mA, respectively. The Cu-Kα radiation was applied to record the XRD graphs between the 2Θ angles of 5° and 30°.

#### 2.2.9. Differential scanning calorimeter

The thermal characteristic of Curcumin powder, HP-β-CyD and HP-γ-CyD webs, Curcumin/HP-β-CyD and Curcumin/HP-γ-CyD webs, Curcumin/HP-β-CyD, and Curcumin/HP-γ-CyD physical mixtures were investigated using differential scanning calorimeter (DSC, Q2000, TA Instruments, USA). The samples were accurately weighted and sealed into Tzero aluminium pan just before the DSC measurements. The samples were subsequently heated from 0 °C to 240 °C with the heating rate of 10 °C/min under the nitrogen atmosphere.

#### 2.2.10. Thermogravimetric analysis

The thermogravimetric profiles of Curcumin powder, HP-β-CyD and HP-γ-CyD webs, Curcumin/HP-β-CyD and Curcumin/HP-γ-CyD webs were examined using thermogravimetric analyzer (TGA, Q500, TA Instruments, USA). For the TGA measurements, a definite weight of sample was located onto platinum TGA pan and heated from room temperature to 600 °C at a heating rate of 20 °C/min under the nitrogen atmosphere.

#### 2.2.11. Dissolution and disintegration studies

In order to evaluate the fast-dissolution profile, ~10 mg of nanofibrous webs of Curcumin/HP-β-CyD and Curcumin/HP-γ-CyD, and

~0.6 mg curcumin powder were put into glass vial, separately. Then, 5 mL of distilled water was poured into these vials while the video was recorded concurrently in order to follow the dissolution. The dissolution profile of Curcumin/HP-β-CyD and Curcumin/HP-γ-CyD physical mixtures having the total sample amount of ~10 mg was examined for comparison.

The disintegration profiles of Curcumin/CyD webs were examined using the slightly modified version of a technique which was reported by Bi et al. (1996). In this technique, the surface of a moist tongue was simulated in terms of physiological conditions. For the experiment, a filter paper with a proper size was located in a plastic petri dish (10 cm) and then wetted with 10 mL of artificial saliva (1.19 g $Na_2HPO_4$, 0.095 g $KH_2PO_4$ and 4 g NaCl were dissolved in 500 mL distilled water, pH was arranged as 6.8 by the addition of phosphoric acid). The excess artificial saliva was subsequently drained from the petri dish and a piece of Curcumin/CyD web (~1.5 cm X 3.0 cm) was placed at the centre of the filter paper and a video was recorded during the disintegration test.

#### 2.2.12. Solubility and antioxidant activity test

The solubility enhancement of curcumin encapsulated in Curcumin/HP-β-CyD and Curcumin/HP-γ-CyD webs was demonstrated using UV–Vis spectroscopy. Here, curcumin powder (~0.6 mg) and Curcumin/CyD webs (~10 mg) were stirred in 5 mL distilled water for 24 h at room temperature and 150 rpm. Then, all aqueous systems were filtered by 0.45 μm PTFE filter to remove the un-dissolved curcumin in the solutions and diluted with PBS (pH 7.4) prior the UV–Vis measurements. UV–Vis absorbances were recorded in the range of 350–650 nm for each sample.

The antioxidant activity of curcumin powder and Curcumin/CyD webs were investigated using 2,2-diphenyl-1-picrylhydrazyl (DPPH) radical scavenging assay. For antioxidant test, ~10 mg webs of Curcumin/HP-β-CyD and Curcumin/HP-γ-CyD, and ~0.6 mg curcumin powder were dissolved in 5 mL of distilled water and then filtered by 0.45 μm PTFE filter to remove the un-dissolved curcumin in the solutions. In the meanwhile, the DPPH solution (75 μM) was freshly prepared in methanol. Afterwards, the aqueous solution of sample and the methanolic DPPH solution was mixed with 1:11 (sample:DPPH) volume ratio (v/v) and incubated in the dark for 1 h. After the incubation, UV–Vis spectroscopy was used to determine the absorbance of solution at 517 nm. For comparison, the same experiment was also performed for pristine HP-β-CyD and HP-γ-CyD webs (~10 mg). For the concentration dependent antioxidant tests, the solution of samples was prepared at nanofibrous web concentration range of 21–333 μg/mL. Each solution was mixed with the DPPH solution (1:11 (sample:DPPH)) and incubated at dark for 1 h. The disappearance of DPPH absorption (517 nm) was examined with UV–Vis spectroscopy. Each experiment was performed in triplicate. The radical scavenging efficiency of Curcumin/CyD webs were calculated in terms of inhibition percentage by using the following equation;

$$\text{Inhibition}\,(\%) = (A_{control} - A_{sample})/A_{control} \times 100 \quad (3)$$

where $A_{control}$ and $A_{sample}$ stand for the absorbance values of control DPPH solution and sample solution, respectively. Additionally, 50% inhibition (IC50) concentrations was calculated from the concentration dependent graph to depict the necessary antioxidant sample amount to decrease the DPPH concentration by 50% (Ak & Gülçin, 2008).

#### 2.2.13. Statistical analyses

The results of the experiments performed at least three replicates, were expressed as mean values and standard deviations. The statistical analyses were carried out by one-way or two-way of variance (ANOVA), whichever was applicable. The ANOVA analyses were done using the OriginLab (Origin 2019, USA) at a 0.05 level of probability.

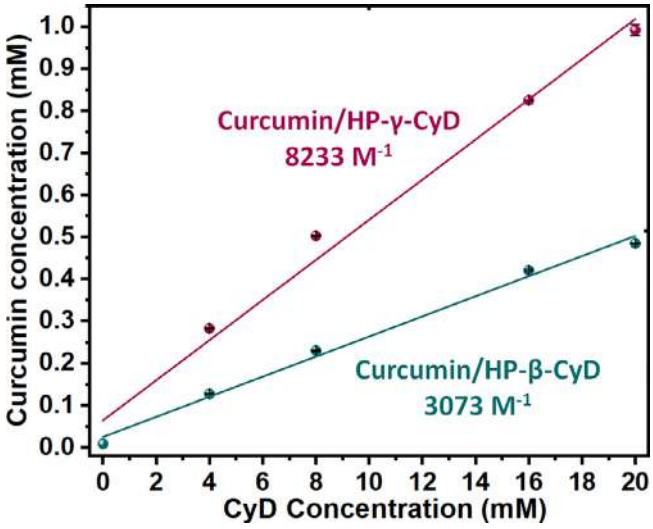


**Fig. 2.** Phase solubility diagram of Curcumin/HP-β-CyD and Curcumin/HP-γ-CyD systems.

## 3. Results and discussion

### 3.1. Phase solubility test

The phase solubility profile of a guest molecule/CyD system gives information on the solubility enhancement of hydrophobic active compound, inclusion stoichiometry and the stability constant (Ks) of the complex (Higuchi & Connors, 1965). In this study, the dynamic equilibrium of Curcumin/CyD systems were reached up to 24 h and UV–Vis measurements were performed from the filtered aliquot of each solution. The phase solubility diagrams of curcumin in the presence of various concentrations of HP-β-CyD and HP-γ-CyD were displayed in Fig. 2. Additionally, the representative UV–Vis spectra of Curcumin/HP-β-CyD and Curcumin/HP-γ-CyD systems were depicted in Fig. S1 which were recorded for the phase solubility analysis. As illustrated in Fig. 2, the aqueous solubility of curcumin increases linearly as a function of both HP-β-CyD and HP-γ-CyD concentrations up to 20 mM which could be classified as $A_L$ type phase solubility diagram according to Higuchi and Connors (Higuchi & Connors, 1965). The linear relationship in the phase solubility diagrams indicates the inclusion complex formation with 1/1 stoichiometry (Higuchi & Connors, 1965). However, curcumin has a symmetric molecular structure with two 3-methoxy 4-hydroxy substituted phenyl moieties (Fig. 1b) and CyD can form inclusion complexes with both 1/1 or 1/2 stoichiometry (Curcumin/CyD) where one or two aromatic moieties is encapsulated in CyD cavity (Singh, Tønnesen, Vogensen, Loftsson, & Másson, 2010; Tomren, Masson, Loftsson, & Tønnesen, 2007). In our case, we have observed $A_L$ type of phase solubility diagram which is consistent with a 1/1 molecular complex formation and this result is coherent with the previous reports in the literature which was performed with a similar CyD concentration range (0–20 mM) and similar experimental details (Li et al., 2018; Syed & Peh, 2013; Yadav et al., 2009). On the other hand, curcumin molecules favorably form 1/2 inclusion complexes with the hydroxypropyl derivates of β-CyD and γ-CyD as it was studied and demonstrated in other related reports (Baglole, Boland, & Wagner, 2005; Singh et al., 2010). Here, the solubility of curcumin was increased by ~57 times with HP-β-CyD and ~123 times with HP-γ-CyD compared to solubility of curcumin in water (~8 μM). The statistical analysis of this experiment has also shown that the means of the two sample are significantly different from each other ($p < 0.05$). The inset photographs given in Fig. S1(a) and (b) also indicated the color change of solutions from transparent to yellow as the concentration of dissolved curcumin increased. In addition, the stability constant (Ks)

values were calculated as 3073 $M^{-1}$ and 8233 $M^{-1}$ for Curcumin/HP-β-CyD and Curcumin/HP-γ-CyD systems, respectively which suggest the stable complex formation between curcumin and CyD and this is essential for enhancing the bioavailability of hydrophobic compounds (Li et al., 2018). Ks value of 3073 $M^{-1}$ determined for Curcumin/HP-β-CyD system is correlated with the previously reported studies in which the Ks values were calculate as 2941 $M^{-1}$ (Li et al., 2018) and 3996 $M^{-1}$ (Syed & Peh, 2013). Unfortunately, Ks value for Curcumin/HP-γ-CyD system could not be attained from the literature which was acquired upon a similar experimental approach and support our results. On the other hand, as Tomren et al. (2007) and Baglole et al. (2005) explained in their studies, curcumin derivates which have side groups on their phenyl moiety indicate higher affinity to HP-γ-CyD due its bigger cavity size compared to HP-β-CyD. Even, HP-γ-CyD provides the greatest solubility enhancement for curcumin molecules among other parent and modified CyD types (Baglole et al., 2005; Tomren et al., 2007). In our case, the significantly higher Ks value and solubilizing effect were also observed for Curcumin/HP-γ-CyD system compared to Curcumin/HP-β-CyD, which is in line with the literature. Our finding suggests that curcumin forms more stable and favourable inclusion complex with HP-γ-CyD compared to HP-β-CyD and therefore HP-γ-CyD provides a better solubility profile for curcumin.

### 3.2. Morphology characterization

Curcumin is a relatively long molecule (Fig. 1b) and it has been shown that curcumin molecules favorably form 1/2 (Curcumin/CyD) inclusion complexes with the hydroxypropyl derivates of β-CyD and γ-CyD (Fig. 1c) (Baglole et al., 2005; Singh et al., 2010). Therefore, we first prepared Curcumin/CyD aqueous solutions having 1/2 M ratio for the electrospinning. Even though 1/2 M ratio of Curcumin/CyD was reported to be optimal inclusion complexation ratio for HP-β-CyD and HP-γ-CyD (Baglole et al., 2005; Singh et al., 2010), the solutions of Curcumin/HP-β-CyD (1/2) and Curcumin/HP-γ-CyD (1/2) were quite heterogeneous and very turbid due to presence of high amount of undissolved/uncomplexed curcumin. Because, very high concentration of Curcumin/CyD solutions (180%, w/v) having very high viscosity hinder the effective mixing of Curcumin/CyD solutions in order to achieve 1/2 M ratio inclusion complexation between curcumin and CyDs (HP-β-CyD and HP-γ-CyD). So, the process of electrospinning for Curcumin/HP-β-CyD (1/2) and Curcumin/HP-γ-CyD (1/2) aqueous systems was not very productive for obtaining nanofibrous webs with low yield under the applied electrospinning parameters and environmental conditions. We further investigated the electrospinning of Curcumin/CyD aqueous solutions by increasing the content of CyD and the Curcumin/CyD aqueous solutions having 1/4 M ratio was found to be optimal for the electrospinning process. The yellowish Curcumin/HP-β-CyD (1/4) solution was still a bit turbid with the indication of presence of some undissolved/uncomplexed curcumin (Fig. 1e (ii), inset) but, Curcumin/HP-γ-CyD (1/4) solution was more homogeneous and darker in color suggesting that curcumin was completely dissolved in water by inclusion complexation (Fig. 1e (iv), inset). Nevertheless, the electrospinning of Curcumin/CyD aqueous solutions having 1/4 M ratio was quite successful in which we were able to electrospun uniform nanofibers of Curcumin/HP-β-CyD (1/4) and Curcumin/HP-γ-CyD (1/4) (Fig. 1f (ii, iv)). The electrospinning process for Curcumin/HP-β-CyD (1/4) and Curcumin/HP-γ-CyD (1/4) aqueous systems was efficient, in which we were able to obtain self-standing and flexible webs (Fig. 1e (ii, iv)). The Curcumin/CyD webs were yellow-colored due to presence of curcumin, yet, Curcumin/HP-γ-CyD web had darker color compared to Curcumin/HP-β-CyD web even both two Curcumin/CyD webs had same amount of curcumin. The color difference of the Curcumin/CyD webs was like their corresponding solutions suggesting that HP-γ-CyD has a better solubilisation effect for curcumin, which was discussed in phase solubility tests of Curcumin/CyD systems. For comparative study, pristine HP-β-CyD and HP-γ-CyD electrospun webs were also produced in which we obtained uniform nanofibers (Fig. 1f (i, iii)) in the form of white color webs having self-standing and flexible character as well (Fig. 1e (i, iii)).

The SEM images clearly confirmed that the pristine CyD webs (HP-β-CyD and HP-γ-CyD) and the Curcumin/CyD webs (Curcumin/HP-β-CyD and Curcumin/HP-γ-CyD) have bead-free morphology with uniform fibrous structure (Fig. 1f). The viscosity and conductivity of the pristine CyD (HP-β-CyD and HP-γ-CyD) solutions and the Curcumin/CyD (Curcumin/HP-β-CyD and Curcumin/HP-γ-CyD) solutions, and the average fiber diameter (AFD) of these webs are given in Table S1. In electrospinning, solutions having lower viscosity and higher conductivity resulted in thinner fibers since the jet is subjected to more stretching during the electrospinning process (Uyar & Besenbacher, 2008). The electrospinning of pristine HP-β-CyD resulted in nanofibers having AFD of 220 ± 60 nm, whereas the electrospinning of pristine HP-γ-CyD resulted in much thicker fibers mostly in micron scale having AFD of 1260 ± 245 nm, since HP-β-CyD solution has lower viscosity and higher conductivity than the HP-γ-CyD solution (Table S1). Similarly, Curcumin/HP-β-CyD web has AFD of 165 ± 65 nm whereas Curcumin/HP-γ-CyD web has AFD of 940 ± 400 nm. The Curcumin/CyD (Curcumin/HP-β-CyD and Curcumin/HP-γ-CyD) aqueous solutions have lower viscosity and higher conductivity than their pristine CyD (HP-β-CyD and HP-γ-CyD) solutions, hence the electrospinning resulted in fibers with smaller AFD for Curcumin/CyD systems compared to their pristine CyDs. The statistical analysis has also indicated that the variations between samples are significantly different from each other ($p < 0.05$). Furthermore, the uncomplexed curcumin crystals were not seen in SEM images of Curcumin/HP-β-CyD (Fig. 1f (ii)) suggesting that the curcumin crystals were possibly in very small sizes distributed within the fiber matrix.

### 3.3. Structural characterization

$^1$H NMR is a confidential approach in order to calculate the molar ratio between guest molecules and CyD and therefore, $^1$H NMR measurements were performed to determine the molar ratio between curcumin and CyD in Curcumin/HP-β-CyD and Curcumin/HP-γ-CyD webs. The electrospinning solutions of Curcumin/CyD systems were prepared by the initial molar ratio of 1/4 for both Curcumin/HP-β-CyD and Curcumin/HP-γ-CyD, however there might be some loss of curcumin during preparation step or electrospinning process. Prior the $^1$H NMR measurements, Curcumin powder, Curcumin/HP-β-CyD web and Curcumin/HP-γ-CyD web were dissolved in *d6*-DMSO and the taken spectra of the samples were depicted in Fig. S2. The molar ratio between curcumin and CyD was calculated by integrating the proportion of the specific peaks of curcumin and CyD in Curcumin/HP-β-CyD and Curcumin/HP-γ-CyD webs. The curcumin peaks between 6.50 and 8.00 ppm and $-CH_3$ group (1.03 ppm) in modified CyDs (HP-β-CyD and HP-γ-CyD) were used for the calculation of molar ratio in these samples. The molar ratio of Curcumin/CyD was calculated as ~1/4 for both Curcumin/HP-β-CyD and Curcumin/HP-γ-CyD webs from the $^1$H NMR peak integrations. The $^1$H NMR analyses demonstrated that the curcumin molecules were effectively encapsulated, and the initial molar ratio of 1/4 was totally preserved for Curcumin/CyD webs during the electrospinning process. It is crucial to state that, Curcumin/HP-β-CyD and Curcumin/HP-γ-CyD webs have the same curcumin peaks with pure curcumin powder that elucidated that the chemical structure of curcumin was protected during the electrospinning process and this is important for the antioxidant activity of curcumin as we mentioned in the following section. The encapsulation efficiency (%) (EE) of Curcumin/CyD webs was further calculated by dissolving samples in the organic solvent of DMSO and the EE was determined as 99.3 ± 1.0% and 98.8 ± 1.6% for Curcumin/HP-β-CyD and Curcumin/HP-γ-CyD webs, respectively using Equation (2). The statistical analysis has also shown that the means of the two sample are not significantly different from each other ($p > 0.05$). These findings are correlated with the $^1$H

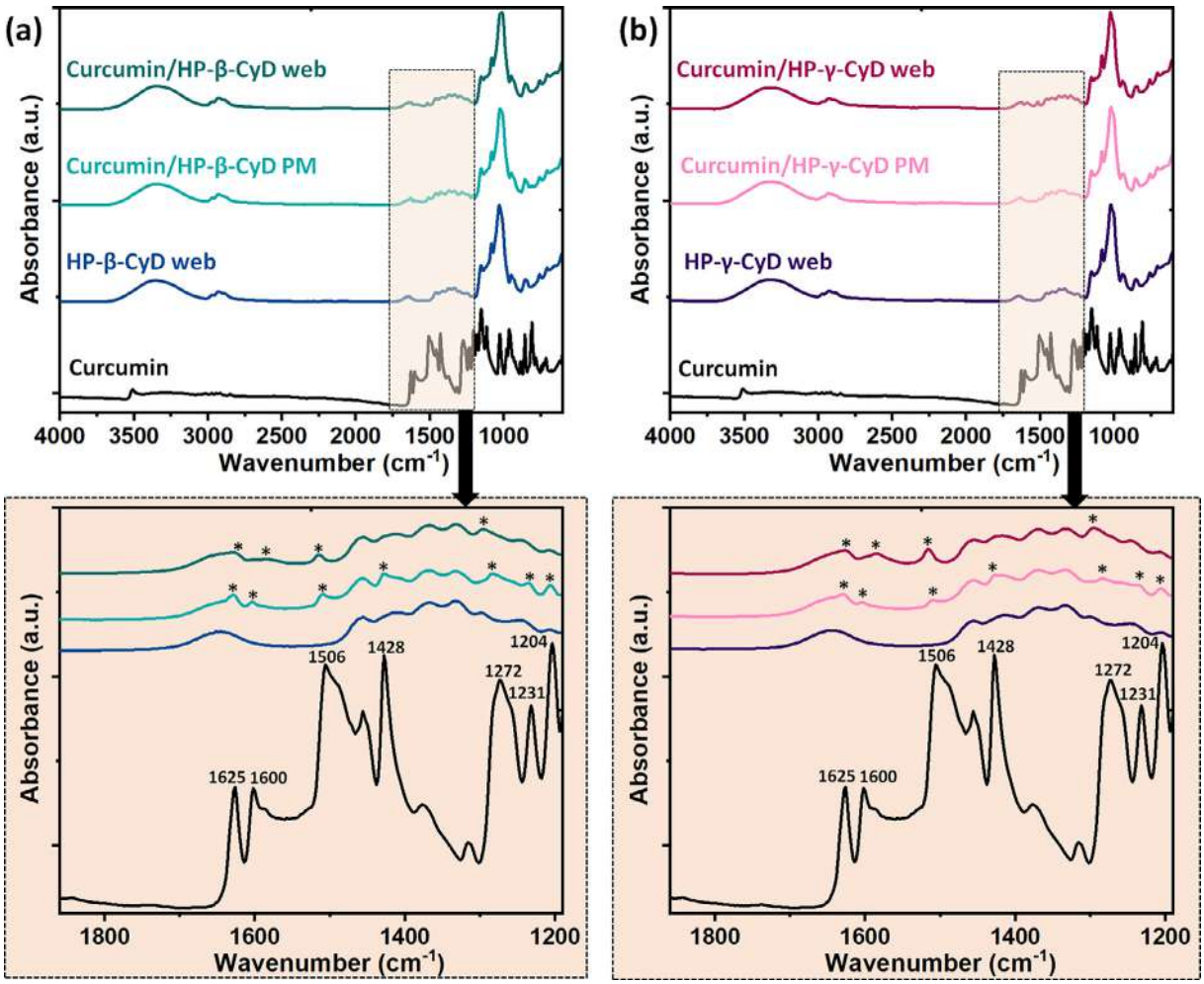


**Fig. 3.** The full and expanded range FT-IR spectra of (a) Curcumin, HP-β-CyD web, Curcumin/HP-β-CyD physical mixture (PM) and Curcumin/HP-β-CyD web, (b) Curcumin, HP-γ-CyD web, Curcumin/HP-γ-CyD physical mixture (PM) and Curcumin/HP-γ-CyD web.

NMR measurements in which the molar ratio of Curcumin/CyD webs was calculated as ~1/4 which corresponds to the ~100% encapsulation efficiency value and ~6% (w/w, with respect to total sample amount) loading capacity for both electrospun webs.

FT-IR is one of the most readily applied techniques in order to ascertain the existence of guest molecules in inclusion complex structure and the inclusion complex formation between CyD and guest molecules (Celebioglu & Uyar, 2019). Such that, the interaction of guest molecules with CyD cavities could lead to shifts, disappearance and/or attenuation in the characteristic peaks of guest molecules (Narayanan, Boy, Gupta, & Tonelli, 2017). The FT-IR spectra of Curcumin powder, HP-β-CyD and HP-γ-CyD webs, Curcumin/HP-β-CyD and Curcumin/HP-γ-CyD webs, Curcumin/HP-β-CyD, and Curcumin/HP-γ-CyD physical mixtures are depicted in Fig. 3. In the full range FT-IR spectra, there are prominent peaks at around 3000–3600, 2930, 1650 and 1370 $cm^{-1}$ corresponds to the primary/secondary –OH stretching, C—H stretching, O—H bending and $–CH_3$ bending vibrations of CyD, respectively. The other prominent absorption bands which are observed at 1028, 1150 and 1180 $cm^{-1}$ owing to vibrations of coupled C—C/C—O stretching and antisymmetric C—O—C glycosidic bridge stretching of CyD (Celebioglu & Uyar, 2019) (Fig. 3). The higher content of CyD in the Curcumin/CyD webs makes it difficult to obtain information about the inclusion complexation from the region of 1000–1200 $cm^{-1}$ since CyD and curcumin peaks are overlapped, and the characteristic peaks of curcumin are inherently masked by the CyD peaks. Nonetheless, there are obvious absorption peaks of curcumin at FT-IR spectra of Curcumin/CyD webs at 1272, 1506, 1600 and 1625 $cm^{-1}$ which are respectively attributed to the aromatic C—O/C—C stretching, benzene ring vibration, aromatic C═C stretching and C═O stretching (Gumireddy et al., 2019). This finding proved the presence of curcumin in samples of Curcumin/CyD webs (Fig. 3). As it was previously reported, both benzene rings of curcumin can be encapsulated in the CyD cavity by van der Waals forces, hydrophobic interactions and hydrogen bonds (Fig. 1c) (Baglole et al., 2005; Mangolim et al., 2014). These interactions can lead to some shifts to lower and/or higher wavenumber of curcumin characteristic peaks at the FT-IR spectra (Mangolim et al., 2014). Here, we have detected shifts for the peaks of curcumin, that is, the peaks at 1272 $cm^{-1}$, 1506 $cm^{-1}$ and 1600 $cm^{-1}$ were shifted to the 1295 $cm^{-1}$, 1516 $cm^{-1}$ and 1584 $cm^{-1}$, respectively and these peaks correspond to the aromatic C—O/C—C stretching, benzene ring vibration, aromatic C═C stretching of curcumin, respectively. This observation proved the inclusion complex formation between curcumin and CyD by entry of aromatic rings of curcumin into CyD cavities in Curcumin/CyD webs. On the other hand, no shift was observed for the same peaks of curcumin in Curcumin/CyD physical mixtures (Fig. 3a–b). Additionally, some of the characteristic peaks of curcumin became more obvious in case of Curcumin/CyD physical mixtures because of the uncomplexed state of curcumin in these samples (Rafati, Zarrabi, Caldera, Trotta, & Ghias, 2019). To conclude, the FT-IR analyses confirmed both the presence and the inclusion complex formation of curcumin in Curcumin/CyD.

Curcumin is a crystalline molecule and XRD provides useful information whether the curcumin molecules are distributed in the CyD fiber matrix as crystals or as amorphous form. XRD also provides

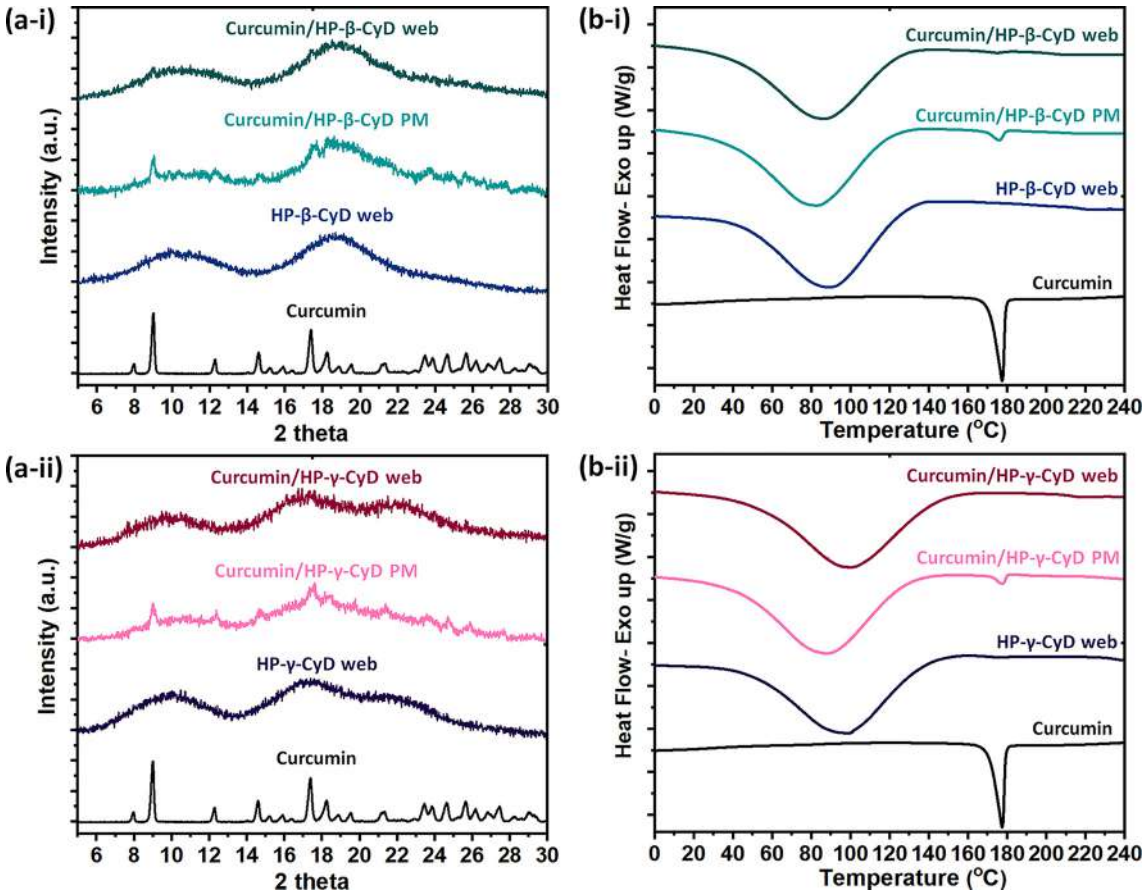


**Fig. 4.** (a) XRD patterns and (b) DSC thermograms of (i) Curcumin, HP-β-CyD web, Curcumin/HP-β-CyD physical mixture (PM) and Curcumin/HP-β-CyD web, (ii) Curcumin, HP-γ-CyD web, Curcumin/HP-γ-CyD physical mixture (PM) and Curcumin/HP-γ-CyD web.

valuable information about the inclusion complexation between CyDs and guest molecules (Narayanan et al., 2017). For instance, when inclusion complex is formed, the guest molecules cannot form its own crystalline aggregates since they are separated from each other by the cavity of CyD. Fig. 4a displays the XRD patterns of electrospun Curcumin/HP-β-CyD web and Curcumin/HP-γ-CyD web. The XRD patterns for Curcumin powder, pristine CyD webs (HP-β-CyD and HP-γ-CyD) and Curcumin/CyD (HP-β-CyD and HP-γ-CyD) physical mixtures were also recorded for a comparison study (Fig. 4a). The as-received curcumin powder is crystalline showing characteristic diffraction pattern having peaks at 8.9° and 17.4° (Fig. 4a) (Mangolim et al., 2014). The hydroxypropylated derivatives (HP-β-CyD and HP-γ-CyD) are amorphous CyD types, so, pristine HP-β-CyD web and HP-γ-CyD web have only broad halo XRD pattern due to their amorphous nature. The Curcumin/HP-β-CyD web and Curcumin/HP-γ-CyD web have also broad halo XRD pattern similar to that of pristine CyD webs (HP-β-CyD and HP-γ-CyD). Yet, the XRD pattern of Curcumin/HP-β-CyD web has shown very weak characteristic diffraction peaks (8.9° and 17.4°) of curcumin indicating that there was some amount of curcumin crystal in this sample (Fig. 4a (i)). On the other hand, curcumin was totally in the inclusion complex state in Curcumin/HP-γ-CyD web (Fig. 4a (ii)). The XRD findings correlate with the visual observation of the Curcumin/CyD solutions where the Curcumin/HP-β-CyD solution was turbid because of the undissolved curcumin crystals whereas the Curcumin/HP-γ-CyD solution was clear without showing any sign of undissolved curcumin crystals. Even though the Curcumin/CyD physical mixtures have same amount of curcumin with Curcumin/CyD webs, the curcumin peaks are prominently obvious in case of physical mixture because of the uncomplexed state of curcumin (Fig. 4a).

We further performed DSC studies to detect if there was any presence of uncomplexed crystalline curcumin in Curcumin/CyD web samples. The DSC data shows that curcumin is crystalline having a melting peak at 177 °C (Fig. 4b). The pristine HP-β-CyD web and HP-γ-CyD web don't have any melting endotherm since they are amorphous, but, DSC data show broad endothermic peak for water loss between 30 and 140 °C (Celebioglu & Uyar, 2019). The DSC data of Curcumin/HP-β-CyD web has a very small endothermic peak at 174 °C for melting of curcumin crystals with a peak area of ~1.1 J/g (Fig. 4b (i)). The physical mixture of Curcumin/HP-β-CyD prepared for comparison has endothermic peak at 177 °C with a peak area of 4.7 J/g (Fig. 4b (i)). The amount of curcumin was the same for Curcumin/HP-β-CyD web and physical mixture of Curcumin/HP-β-CyD, yet, the melting peak area for Curcumin/HP-β-CyD web was ~75% less than the melting peak area for Curcumin/HP-β-CyD physical mixture indicating that most of the curcumin was inclusion complexed with HP-β-CyD, but, there was still some (~25%) uncomplexed curcumin crystals present in Curcumin/HP-β-CyD web. For Curcumin/HP-γ-CyD, no melting peak was detected for curcumin confirming the fully inclusion complexed state of curcumin with HP-γ-CyD in this sample (Fig. 4b (ii)). On the other hand, the DSC of Curcumin/HP-γ-CyD physical mixture has endothermic peak at 177 °C with a peak area of 4.4 J/g (Fig. 4b (i)). For CyD inclusion complexes, typically the melting of guest molecule is not observed in DSC since guest molecules cannot form crystals as they are separated from each other by CyD cavity (Narayanan et al., 2017). The DSC data are in good agreement with the FT-IR, XRD data and the visual appearance of the Curcumin/CyD solutions. The DSC findings further indicated that curcumin was fully inclusion complexed in Curcumin/HP-γ-CyD web whereas there was some amount of uncomplexed crystalline curcumin present in Curcumin/HP-β-CyD web.

The TGA measurements of Curcumin powder, pristine HP-β-CyD

and HP-γ-CyD webs, Curcumin/HP-β-CyD and Curcumin/HP-γ-CyD webs were carried out by the thermo-analytic analyses (Fig. S3). The curcumin powder displays mass loss that starts at 145 °C and ends up at 500 °C. The pristine HP-β-CyD web and HP-γ-CyD web samples exhibit initial weight (%) loss below 100 °C due to the evaporation of water. The main thermal degradation of pristine HP-β-CyD web and HP-γ-CyD web occurs between 280 and 430 °C and 265–420 °C, respectively. As seen in Fig. S3a (ii)–b (ii), the main degradation of curcumin overlaps with the main degradation step of pristine CyD. Therefore, two steps of mass losses were also observed for Curcumin/HP-β-CyD web and Curcumin/HP-γ-CyD web. Even so, the derivative curve of CyD webs got wider and reduced in intensity in case of Curcumin/CyD webs owing to the curcumin content in these samples (Fig. S3a (ii)–b (ii)). Such that, the main degradation of HP-β-CyD and HP-γ-CyD starts at 280 °C and 265 °C, respectively and they shift to lower temperature of ~250 °C for both Curcumin/HP-β-CyD web and Curcumin/HP-γ-CyD web. Fundamentally, it is also possible to determine the weight ratios of each component in these samples by TGA method. However, the degradation step of curcumin was totally buried under the main degradation of CyD in case of both Curcumin/CyD webs (Fig. S3) which makes it difficult to calculate the content of curcumin in Curcumin/CyD webs from TGA results. Principally, the increase in thermal stability of guest molecules is considered as an evidence of inclusion complexation (Narayanan et al., 2017). In this study, TGA findings demonstrated the interaction between curcumin and CyD in Curcumin/CyD webs in terms of altered the degradation profile of CyD molecules.

### 3.4. Dissolution and disintegration profile of Curcumin/CyD webs

The fast dissolution of Curcumin/CyD webs (~10 mg) was visually investigated by adding 5 mL of water to the glass vials (Fig. 5a, Video S1). For comparison, pure curcumin powder (~0.6 mg) was tested, as well. Here, Curcumin/CyD webs immediately disappeared with the addition of water. However, curcumin powder remained on the top of water surface and did not dissolve over this period because of its almost insoluble nature (Fig. 5a). The fast-dissolution test demonstrated that, there are uncomplexed curcumin in Curcumin/HP-β-CyD web, since Curcumin/HP-β-CyD web solution is not clear as Curcumin/HP-γ-CyD web solution. As seen in Fig. 5a, the solution of Curcumin/HP-γ-CyD web simultaneously became clear by the dissolution of web, however there are still undissolved curcumin parts in solution of Curcumin/HP-β-CyD web because of the uncomplexed/crystalline curcumin content in Curcumin/HP-β-CyD web. Here, Curcumin/CyD webs were produced with the molar ratio of 1/4 (Curcumin/CyD) since this molar ratio enabled to obtain Curcumin/CyD webs with the homogenous morphology and high yield. On the other hand, the high concentration of CyD (180%, w/v), required for the electrospinning of defect-free nanofibers, was one of the drawback during the preparation of electrospinning solution of Curcumin/CyD system, because the high viscosity of CyD solutions made difficult the effluent stirring of systems in order to form inclusion complexes. But, the use of high concentration of CyD for electrospinning also provides much higher fiber production rate as compared to polymeric systems. Here, the process was optimized in terms of concentration, molar ratio, process time and temperature etc. to attain the most efficient and adoptable results for both CyD types. Despite all, as it was addressed in phase solubility part, curcumin forms less favourable complexes with HP-β-CyD compared to HP-γ-CyD which most probably induced less efficient inclusion complex formation in the highly concentrated and viscous solution of Curcumin/HP-β-CyD. Nevertheless, the fast-dissolving character was observed for Curcumin/HP-γ-CyD web resulting complete dissolution and clear solutions without any indication of undissolved curcumin. Here, the dissolution profile of Curcumin/CyD physical mixtures has been examined, as well (Video S2) and it was observed that the curcumin parts separate from the constitution of the physical mixture with the addition of water and could not dissolve effectively because of their uncomplexed state.

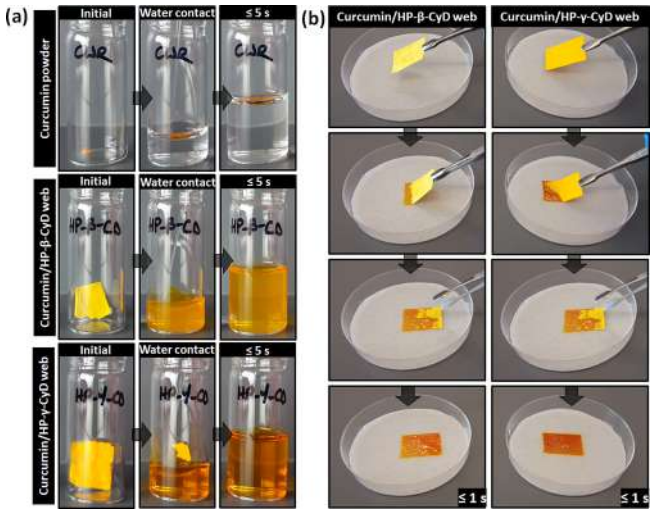


**Fig. 5.** (a) The dissolution behavior of Curcumin powder, Curcumin/HP-β-CyD web and Curcumin/HP-γ-CyD webs in distilled water. (b) The disintegration behavior of Curcumin/HP-β-CyD web and Curcumin/HP-γ-CyD webs at the artificial saliva environment. The pictures were captured from the videos which were given as Video S1 and Video S3.

The disintegration of Curcumin/CyD webs was further investigated using wet filter paper to simulate the moist environment of oral cavity (Bi et al., 1996). Fig. 5b and Video S3 depict the disintegration profile of Curcumin/CyD webs. Both Curcumin/HP-β-CyD and Curcumin/HP-γ-CyD webs were immediately adsorbed by artificial saliva and dissolved rapidly. Even, there are uncomplexed/crystalline curcumin in Curcumin/HP-β-CyD web, this situation did not reflect on the disintegration test results and both nanofibrous webs indicated similar disintegration profile. The hydroxypropylated derivates of HP-β-CyD and HP-γ-CyD are highly water soluble CyD types and it is a crucial dynamic for the high dissolution and disintegration rate of Curcumin/CyD webs (Loftsson & Brewster, 2010). In addition, highly porous structure and high surface area of nanofibrous webs are other influential properties which guarantee actual penetration path and interaction sides for water through the nanofibers in the course of dissolution and disintegration of webs (Yu et al., 2018). Briefly, nanoporous structure of Curcumin/CyD webs can enable the easy penetration of saliva in the mouth, the high-water solubility of modified CyD (HP-β-CyD and HP-γ-CyD) and inclusion complexation between curcumin and CyD can provide rapid release of curcumin by very fast-dissolution of Curcumin/CyD nanofibrous webs.

### 3.5. Solubility and antioxidant activity test

The solubility improvement of curcumin in Curcumin/CyD webs was also proved by the UV–Vis spectroscopy measurement. Fig. 6a indicated the UV–Vis absorbance spectra of the solution of Curcumin powder, Curcumin/HP-β-CyD web and Curcumin/HP-γ-CyD web. As is seen, pure Curcumin solution did not have an obvious absorbance peak at the specific wavelength of curcumin (430 nm), because of its extremely poor solubility (~8 μM) which is also supported by the almost colorless solution (Fig. 6a-inset). Even, the solutions of Curcumin/HP-β-CyD and Curcumin/HP-γ-CyD webs were prepared having the same amount of curcumin (~0.5 mg), the absorption intensity of Curcumin/CyD webs was much higher than the pure Curcumin solution clearly showing that the water solubility of curcumin was significantly improved in case of Curcumin/CyD webs due to inclusion complexation. Moreover, the absorption intensity of Curcumin/HP-γ-CyD solution is significantly higher compared to Curcumin/HP-β-CyD solution (Fig. 6a). This result further confirms that Curcumin/HP-γ-CyD web is superior than Curcumin/HP-β-CyD web for enhancing the water

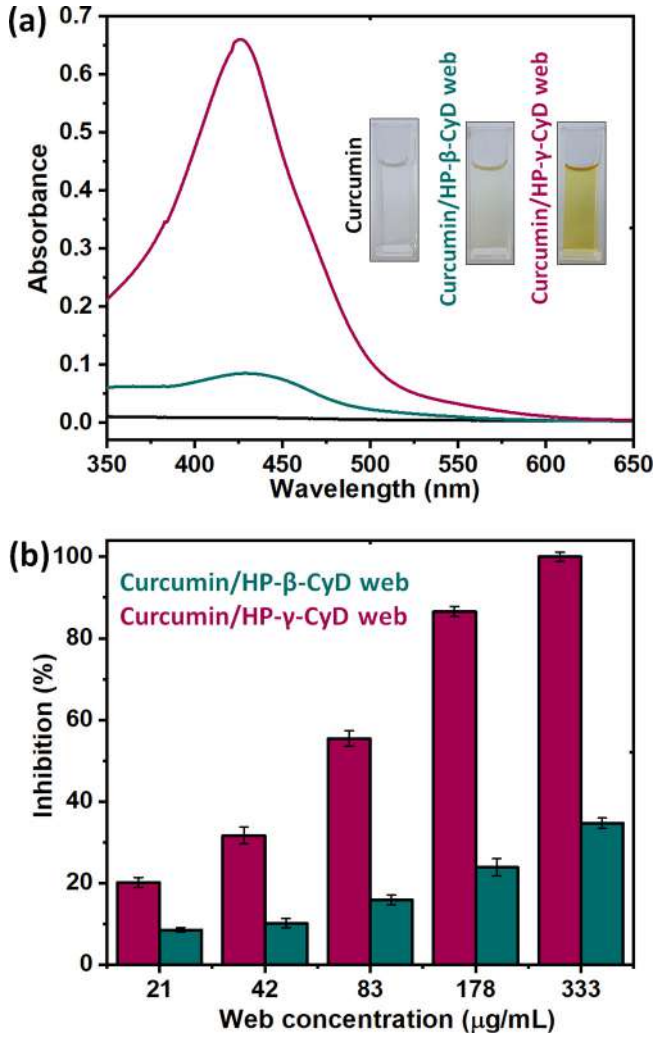


**Fig. 6.** (a) UV–Vis spectra and the photographs of the aqueous solutions of Curcumin, Curcumin/HP-β-CyD web and Curcumin/HP-γ-CyD web. (b) Concentration dependent antioxidants performance graphs of Curcumin/HP-β-CyD web and Curcumin/HP-γ-CyD web.

solubility of curcumin. The darker yellow color of the solution of Curcumin/HP-γ-CyD web is an indicator, as well, for the higher amount of dissolved curcumin in the solution (Fig. 6a). As addressed in FT-IR, XRD and DSC analyses, there was uncomplexed/crystalline curcumin part in the Curcumin/HP-β-CyD web which could not be dissolved and therefore filtered out, hence, the intensity of the UV–Vis spectrum is significantly lower than the solution of Curcumin/HP-γ-CyD web. The findings are correlated with the phase solubility results in which the HP-γ-CyD has higher solubility increase for curcumin (~123 times) than the HP-β-CyD (~57 times).

Free radicals and reactive oxygen species (ROS) can cause or induce different human pathologies such as; stroke, cancer, neurodegenerative diseases upon the oxidation of various biomolecules (DNA, proteins, lipids etc.) (Gülçin, 2012). Antioxidant compounds are supposed to inhibit the destructive effects of free radicals and ROS by scavenging them (Gülçin, 2012). The antioxidant activity of curcumin mainly depends on proton loss from the phenolic OH group along with the phenoxyl radical formation (Ak & Gülçin, 2008). In case of dimethoxy curcumin, the phenolic OH can be blocked by the methoxy moieties and the loss of hydrogen from the heptadienone linkage between the two methoxyphenol rings become more favourable for the antioxidant activity of curcumin molecules (Ak & Gülçin, 2008). Here, the antioxidant property of curcumin and Curcumin/CyD webs were examined using 2,2-diphenyl-1-picrylhydrazyl (DPPH) scavenging assay. The decrease of the absorbance intensity of DPPH at 517 nm was followed for the evaluation of the antioxidant activity of samples. Fig. S4 shows the radical scavenging test results of pure Curcumin, Curcumin/HP-β-CyD web and Curcumin/HP-γ-CyD web. Since curcumin powder could not dissolve in water, the solution of curcumin could not indicate an antioxidant activity and the almost same absorbance profile was obtained with the DPPH stock solution (Fig. S4). On the other, Curcumin/HP-β-CyD web and Curcumin/HP-γ-CyD web showed 34.7 ± 1.2% and 100 ± 1.0% antioxidant activity, respectively and so, the color of the solution turns into light purple for Curcumin/HP-β-CyD web, and yellow for Curcumin/HP-γ-CyD web. The results revealed that, while Curcumin/HP-γ-CyD web reached to maximum antioxidant activity of ~100%, Curcumin/HP-β-CyD web indicated lower antioxidant performance (~35%) for the same curcumin content and web concentration (333 μg/mL) under the same conditions. As it was also addressed in the solubility test, there is uncomplexed/crystalline curcumin in the Curcumin/HP-β-CyD web which was removed with the filtration and could not take part in the radical scavenging process. The result is compatible with both phase solubility and solubility tests in which lower solubilizing effect was obtained for HP-β-CyD compared to HP-γ-CyD because of lower complexation efficiency of HP-β-CyD with curcumin. The same antioxidant tests procedure was performed for pristine HP-β-CyD and HP-γ-CyD web, however they did not show radical scavenging property (data is not shown). The concentration dependent antioxidant activity tests of Curcumin/HP-β-CyD and Curcumin/HP-γ-CyD web were performed for the web concentration range of 21–333 μg/mL. Fig. 6b displays % DPPH radical inhibition graphs of Curcumin/CyD webs depending on the concentration. As it was expected, the inhibition efficiency of the Curcumin/CyD increased by the increasing Curcumin/CyD web concentration depending on the dose-dependent radical scavenging manner. The concentration dependent inhibition (%) graph enabled to calculate IC50 value which represents the amount of antioxidant material necessary to decrease the initial DPPH radical concentration by 50% (Ak & Gülçin, 2008). The IC50 value was determined as web concentrations of 501 μg/mL and 81 μg/mL for Curcumin/HP-β-CyD and Curcumin/HP-γ-CyD webs, respectively. The lower IC50 of Curcumin/HP-γ-CyD web supported the higher free radical scavenging activity, since less amount of Curcumin/HP-γ-CyD web is needed to display the antioxidant activity compared to Curcumin/HP-β-CyD web. This notable difference is appeared due to the higher complexation efficiency of HP-γ-CyD with curcumin which was also demonstrated in phase solubility and solubility studies. Due to the higher complexation efficiency, higher amount of curcumin became soluble in the Curcumin/HP-γ-CyD web and higher amount curcumin could contribute more to the scavenging of DPPH radical. The statistical analyses of antioxidant test have also revealed that the variations between samples are significant ($p < 0.05$).

## 4. Conclusion

In conclusion, electrospinning technique enable to encapsulate various kind of bioactive agents such as; food supplements, essential oils, vitamins, flavors, etc, into nanofibrous webs. In addition, cyclodextrins (CyDs) can form inclusion complexes with these bioactive compounds and enhance their water solubility, thermal stability and bioavailability. This is why the electrospun CyD inclusion complexes with bioactive compounds is a promising approach for food related applications. Here, the inclusion complex of curcumin was obtained from the highly water soluble derivates of CyD; Hydroxypropyl-beta-Cyclodextrin (HP-β-CyD) and Hydroxypropyl-gamma-Cyclodextrin (HP-γ-CyD). The chosen CyD types were used as both complexation host and fiber matrix in order to enhance the water-solubility and antioxidant activity of curcumin. The inclusion complexation and electrospinning process were optimized to produce defect-free and homogenous inclusion complex nanofibrous webs with ~100% encapsulation

efficiency. The free-standing nanofibrous webs of Curcumin/HP-β-CyD and Curcumin/HP-γ-CyD were obtained successfully. Both HP-β-CyD and HP-γ-CyD were effective for the improved water-solubility of curcumin by forming inclusion complexation, yet, HP-γ-CyD significantly has a much higher solubilizing enhancement for curcumin compared to HP-β-CyD. Curcumin/CyD webs have shown very fast-dissolving profile in water and Curcumin/CyD webs disintegrated immediately when wetted with artificial saliva. Additionally, Curcumin/CyD webs provided a prominent enhancement in antioxidant property of curcumin. It is also worth to mention that, the electrospinning of Curcumin/CyD nanofibrous webs was performed in water and this offers advantage for the industrial processing and the commercialization of the active compounds/CyD inclusion complex nanofibrous webs. In short, our study shows that Curcumin/CyD nanofibrous webs have various advantages coming from both electrospinning technique and cyclodextrin. This novel design can be considered as a promising step in food technology and can pave of the way of development for orally fast-dissolving strips/webs as food supplements.

## CRediT authorship contribution statement

**Asli Celebioglu:** Methodology, Validation, Investigation, Writing - original draft, Writing - review & editing. **Tamer Uyar:** Supervision, Resources, Methodology, Writing - original draft, Project administration, Funding acquisition.

## Declaration of Competing Interest

The authors declare that they have no known competing financial interests or personal relationships that could have appeared to influence the work reported in this paper.

## Acknowledgment

This work made use of the Cornell Center for Materials Research Shared Facilities which are supported through the NSF MRSEC program (DMR-1719875), and the Cornell Chemistry NMR Facility supported in part by the NSF MRI program (CHE-1531632), and the Department of Fiber Science & Apparel Design facilities. Prof. Uyar acknowledges the startup funding from the College of Human Ecology at Cornell University. The partial funding for this research was also graciously provided by Nixon Family (Lea and John Nixon) thru College of Human Ecology at Cornell University.

## Author contribution

T. U. and A.C. designed the study. A.C. performed the experimental studies. A.C. and T. U. wrote the manuscript and have given approval to the final version of the manuscript.

## Appendix A. Supplementary data

Supplementary data to this article can be found online at https://doi.org/10.1016/j.foodchem.2020.126397.

## References

Ak, T., & Gülçin, İ. (2008). Antioxidant and radical scavenging properties of curcumin. *Chemico-Biological Interactions, 174*(1), 27–37.

Alehosseini, A., Gómez-Mascaraque, L. G., Martínez-Sanz, M., & López-Rubio, A. (2019). Electrospun curcumin-loaded protein nanofiber mats as active/bioactive coatings for food packaging applications. *Food Hydrocolloids, 87*, 758–771.

Amiri, S., & Rahimi, A. (2019). Poly (ε-caprolactone) electrospun nanofibers containing curcumin nanocontainers: Enhanced solubility, dissolution and physical stability of curcumin via formation of inclusion complex with cyclodextrins. *International Journal of Polymeric Materials and Polymeric Biomaterials, 68*(11), 669–679.

Aytac, Z., & Uyar, T. (2017). Core-shell nanofibers of curcumin/cyclodextrin inclusion complex and polylactic acid: Enhanced water solubility and slow release of curcumin. *International Journal of Pharmaceutics, 518*(1–2), 177–184.

Aytac, Z., Yildiz, Z. I., Kayaci-Senirmak, F., Tekinay, T., & Uyar, T. (2017). Electrospinning of cyclodextrin/linalool-inclusion complex nanofibers: Fast-dissolving nanofibrous web with prolonged release and antibacterial activity. *Food Chemistry, 231*, 192–201.

Baglole, K. N., Boland, P. G., & Wagner, B. D. (2005). Fluorescence enhancement of curcumin upon inclusion into parent and modified cyclodextrins. *Journal of Photochemistry and Photobiology A: Chemistry, 173*(3), 230–237.

Bhushani, J. A., & Anandharamakrishnan, C. (2014). Electrospinning and electrospraying techniques: Potential food based applications. *Trends in Food Science & Technology, 38*(1), 21–33.

Bi, Y., Sunada, H., Yonezawa, Y., Danjo, K., Otsuka, A., & Iida, K. (1996). Preparation and evaluation of a compressed tablet rapidly disintegrating in the oral cavity. *Chemical and Pharmaceutical Bulletin, 44*(11), 2121–2127.

Celebioglu, A., Kayaci-Senirmak, F., İpek, S., Durgun, E., & Uyar, T. (2016). Polymer-free nanofibers from vanillin/cyclodextrin inclusion complexes: High thermal stability, enhanced solubility and antioxidant property. *Food & Function, 7*(7), 3141–3153.

Celebioglu, A., & Uyar, T. (2017). Antioxidant vitamin E/cyclodextrin inclusion complex electrospun nanofibers: Enhanced water solubility, prolonged shelf life, and photostability of vitamin E. *Journal of Agricultural and Food Chemistry, 65*(26), 5404–5412.

Celebioglu, A., & Uyar, T. (2019). Fast dissolving oral drug delivery system based on electrospun nanofibrous webs of cyclodextrin/ibuprofen inclusion complex nanofibers. *Molecular Pharmaceutics*.

Celebioglu, A., Yildiz, Z. I., & Uyar, T. (2018). Fabrication of electrospun eugenol/cyclodextrin inclusion complex nanofibrous webs for enhanced antioxidant property, water solubility, and high temperature stability. *Journal of Agricultural and Food Chemistry, 66*(2), 457–466.

Deng, L., Kang, X., Liu, Y., Feng, F., & Zhang, H. (2017). Effects of surfactants on the formation of gelatin nanofibres for controlled release of curcumin. *Food Chemistry, 231*, 70–77.

Dias, M. I., Ferreira, I. C. F. R., & Barreiro, M. F. (2015). Microencapsulation of bioactives for food applications. *Food & Function, 6*(4), 1035–1052.

Gülçin, I. (2012). Antioxidant activity of food constituents: An overview. *Archives of Toxicology*. https://doi.org/10.1007/s00204-011-0774-2.

Gumireddy, A., Christman, R., Kumari, D., Tiwari, A., North, E. J., & Chauhan, H. (2019). Preparation, characterization, and in vitro evaluation of curcumin-and resveratrol-loaded solid lipid nanoparticles. *AAPS PharmSciTech, 20*(4), 145.

Higuchi, T., & Connors, K. A. (1965). Phase solubility diagram. *Advances in Analytical Chemistry and Instrumentation, 4*, 117–212.

Jahed, V., Zarrabi, A., Bordbar, A., & Hafezi, M. S. (2014). NMR (1H, ROESY) spectroscopic and molecular modelling investigations of supramolecular complex of β-cyclodextrin and curcumin. *Food Chemistry, 165*, 241–246.

Leidy, R., & Ximena, Q.-C. M. (2019). Use of electrospinning technique to produce nanofibres for food industries: A perspective from regulations to characterisations. *Trends in Food Science & Technology*.

Li, N., Wang, N., Wu, T., Qiu, C., Wang, X., Jiang, S., ... Wang, T. (2018). Preparation of curcumin-hydroxypropyl-β-cyclodextrin inclusion complex by cosolvency-lyophilization procedure to enhance oral bioavailability of the drug. *Drug Development and Industrial Pharmacy, 44*(12), 1966–1974.

Loftsson, T., & Brewster, M. E. (2010). Pharmaceutical applications of cyclodextrins: Basic science and product development. *Journal of Pharmacy and Pharmacology, 62*(11), 1607–1621.

Maharjan, P., Jin, M., Kim, D., Yang, J., Maharjan, A., Shin, M. C., ... Min, K. A. (2019). Evaluation of epithelial transport and oxidative stress protection of nanoengineered curcumin derivative-cyclodextrin formulation for ocular delivery. *Archives of Pharmacal Research*, 1–17.

Mangolim, C. S., Moriwaki, C., Nogueira, A. C., Sato, F., Baesso, M. L., Neto, A. M., & Matioli, G. (2014). Curcumin–β-cyclodextrin inclusion complex: Stability, solubility, characterisation by FT-IR, FT-Raman, X-ray diffraction and photoacoustic spectroscopy, and food application. *Food Chemistry, 153*, 361–370.

Marques, H. M. C. (2010). A review on cyclodextrin encapsulation of essential oils and volatiles. *Flavour and Fragrance Journal, 25*(5), 313–326.

Narayanan, G., Boy, R., Gupta, B. S., & Tonelli, A. E. (2017). Analytical techniques for characterizing cyclodextrins and their inclusion complexes with large and small molecular weight guest molecules. *Polymer Testing, 62*, 402–439.

Pankongadisak, P., Sangklin, S., Chuysinuan, P., Suwantong, O., & Supaphol, P. (2019). The use of electrospun curcumin-loaded poly (L-lactic acid) fiber mats as wound dressing materials. *Journal of Drug Delivery Science and Technology*.

Rafati, N., Zarrabi, A., Caldera, F., Trotta, F., & Ghias, N. (2019). Pyromellitic dianhydride crosslinked cyclodextrin nanosponges for curcumin controlled release; formulation, physicochemical characterization and cytotoxicity investigations. *Journal of Microencapsulation, 36*(8), 715–727.

Rauf, A., Imran, M., Orhan, I. E., & Bawazeer, S. (2018). Health perspectives of a bioactive compound curcumin: A review. *Trends in Food Science & Technology, 74*, 33–45.

Singh, R., Tønnesen, H. H., Vogensen, S. B., Loftsson, T., & Másson, M. (2010). Studies of curcumin and curcuminoids. XXXVI. The stoichiometry and complexation constants of cyclodextrin complexes as determined by the phase-solubility method and UV–Vis titration. *Journal of Inclusion Phenomena and Macrocyclic Chemistry, 66*(3–4), 335–348.

Stanić, Z. (2018). Improving therapeutic effects of curcumin-a review. *Journal of Food & Nutrition Research, 57*(2).

Sun, Y., Du, L., Liu, Y., Li, X., Li, M., Jin, Y., & Qian, X. (2014). Transdermal delivery of the in situ hydrogels of curcumin and its inclusion complexes of hydroxypropyl-β-cyclodextrin for melanoma treatment. *International Journal of Pharmaceutics, 469*(1), 31–39.

Syed, H. K., & Peh, K. K. (2013). Comparative curcumin solubility enhancement study of

beta-cyclodextrin (beta CD) and its derivative hydroxypropyl-beta-cyclodextrin (HP beta CD). *Latin American Journal of Pharmacy, 32*(1), 52–59.

Tomren, M. A., Masson, M., Loftsson, T., & Tønnesen, H. H. (2007). Studies on curcumin and curcuminoids: XXXI. Symmetric and asymmetric curcuminoids: Stability, activity and complexation with cyclodextrin. *International Journal of Pharmaceutics, 338*(1–2), 27–34.

Torres-Giner, S., Busolo, M., Cherpinski, A., & Lagaron, J. M. (2018). Electrospinning in the packaging industry. *Electrospinning* (pp. 238–260). .

Uyar, T., & Besenbacher, F. (2008). Electrospinning of uniform polystyrene fibers: The effect of solvent conductivity. *Polymer, 49*(24), 5336–5343.

Wang, L., Mu, R.-J., Li, Y., Lin, L., Lin, Z., & Pang, J. (2019). Characterization and antibacterial activity evaluation of curcumin loaded konjac glucomannan and zein nanofibril films. *LWT*108293.

Yadav, V. R., Suresh, S., Devi, K., & Yadav, S. (2009). Effect of cyclodextrin complexation of curcumin on its solubility and antiangiogenic and anti-inflammatory activity in rat colitis model. *Aaps Pharmscitech, 10*(3), 752.

Yildiz, Z. I., Celebioglu, A., Kilic, M. E., Durgun, E., & Uyar, T. (2018). Menthol/cyclodextrin inclusion complex nanofibers: Enhanced water-solubility and high-temperature stability of menthol. *Journal of Food Engineering, 224*, 27–36.

Yildiz, Z. I., Kilic, M. E., Durgun, E., & Uyar, T. (2019). Molecular encapsulation of cinnamaldehyde within cyclodextrin inclusion complex electrospun nanofibers: Fast-dissolution, enhanced water solubility, high temperature stability and antibacterial activity of cinnamaldehyde. *Journal of Agricultural and Food Chemistry*.

Yu, D.-G., Li, J.-J., Williams, G. R., & Zhao, M. (2018). Electrospun amorphous solid dispersions of poorly water-soluble drugs: A review. *Journal of Controlled Release*.